

# Absorption of terahertz radiation by plasmon modes in a grid-gated double-quantum-well field-effect transistor

V. V. Popov, O. V. Polischuk, and T. V. TeperikX. G. Peralta and S. J. AllenN. J. M. HoringM. C. Wanke

Citation: **94**, 3556 (2003); doi: 10.1063/1.1599051

View online: <http://dx.doi.org/10.1063/1.1599051>

View Table of Contents: <http://aip.scitation.org/toc/jap/94/5>

Published by the [American Institute of Physics](#)

---

---

**AIP** | Journal of  
Applied Physics

**INTRODUCING INVITED PERSPECTIVES**

**Ultrafast magnetism and THz spintronics**

Authors: Jakob Walowski and Markus Münzenberg

# Absorption of terahertz radiation by plasmon modes in a grid-gated double-quantum-well field-effect transistor

V. V. Popov,<sup>a)</sup> O. V. Polischuk, and T. V. Teperik

*Institute of Radio Engineering and Electronics (Saratov Division), Russian Academy of Sciences, Saratov 410019, Russia*

X. G. Peralta and S. J. Allen

*Center for Terahertz Science and Technology, University of California, Santa Barbara, California 93106*

N. J. M. Horing

*Department of Physics and Engineering Physics, Stevens Institute of Technology, Hoboken, New Jersey 07030*

M. C. Wanke

*Sandia National Laboratories, Albuquerque, New Mexico 87185*

(Received 21 January 2003; accepted 18 June 2003)

The terahertz absorption spectrum of plasmon modes in a grid-gated double-quantum-well (DQW) field-effect transistor structure is analyzed theoretically and numerically using a first principles electromagnetic approach and is shown to faithfully reproduce important physical features of recent experimental observations. We find that the essential character of the response—multiple resonances corresponding to spatial harmonics of standing plasmons under the metal grating—is caused by the static spatial modulation of electron density in the channel. Higher order plasmon modes become more optically active as the depth of the electron density modulation in the DQW tends towards unity. The maximum absorbance, at plasma resonance, is shown to be  $1/2$ . Furthermore, the strongest absorption also occurs when the standing plasmon resonance coincides with the fundamental dipole mode of the ungated portion of the channel. © 2003 American Institute of Physics. [DOI: 10.1063/1.1599051]

## I. INTRODUCTION

Recently, the terahertz (THz) photoconductivity of a double-quantum-well (DQW) field-effect transistor (FET) with a periodic metal grid gate (Fig. 1) was observed.<sup>1,2</sup> It appears that the presence of a *double* quantum well is important to produce a strong photoresponse. The positions and the strengths of the peaks in the photoresponse, photoconductance (the change of channel conductance), are controlled by both the voltage,  $V_g$ , applied to the gate and the period of the grating gate. This strongly suggests that the sharply resonant features are related to plasma oscillations in this composite device. The strongest THz photoresponse occurs when the upper QW is fully depleted under metallic portions of the grating gate, while the lower one remains connected, but with laterally modulated electron density. The response is fast (less than 1 ms) and it depends on the presence of the double quantum well channel. Remarkably, the sharpest and strongest resonance response does not occur at the lowest temperatures, but rather between 25 and 40 K. The sign of the photoconductance is not unique, but depends on the grating period. An in-plane magnetic field shifts the resonances towards smaller depletion gate voltages and higher channel densities.<sup>2</sup> It can also reverse the sign of the terahertz photoconductance. The physical mechanism responsible for the THz photoconductivity is not evident at this time. In particu-

lar, the temperature dependence, as well as the reversal of sign of the photoconductance, is not understood.

These experimental results indicate that a grating-gated double-quantum-well field-effect transistor is potentially important as a tunable incoherent detector or coherent (heterodyne) detector in the terahertz regime, particularly with signal processing electronics integrated on the same chip. But further development requires a realistic and physically well-founded model of (i) the electromagnetic interaction of terahertz radiation with the device, the excitation of the plasma resonances, and (ii) the device physics responsible for linking the resonant excitation of the plasmons with a change of dc channel conductance. This article addresses the first aspect of the problem (i), the resonant THz absorption and excitation of plasmons in a grating-gated double-quantum-well field-effect transistor.

A simple “transmission line” model discussed in Ref. 1 that describes plasma oscillations in the grid-gated DQW FET provided a rough qualitative guide and suggested that the series of frequency dependent resonances observed in the THz photoconductance corresponds to the excitation of plasma waves in the structure. However, this simple model fails to explain the measured separation in  $V_g$  between resonances at different frequencies and variation of the line shape with frequency.

Far infrared absorption in density modulated two-dimensional electron systems has been studied theoretically in a series of papers,<sup>3–9</sup> including studies of structures with

<sup>a)</sup>Electronic mail: popov@ire.san.ru

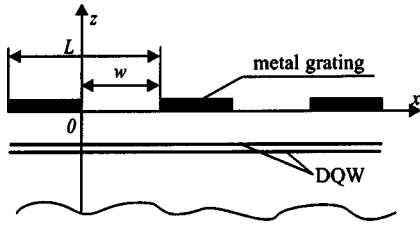


FIG. 1. Schematic of the grid-gated double-quantum-well field-effect transistor structure under consideration.

metal gratings.<sup>4,6,8</sup> In this article we develop a detailed, realistic model of plasmon electrodynamics in the grid-gated DQW FET structure studied experimentally in Ref. 1. In Sec. II we start with the simplest model of a resonant surface electron layer in order to examine the essential physics of energy transformation in the structure. In Sec. III we discuss the plasmon electrodynamics of the model of a single density-modulated two-dimensional electron gas (2DEG) layer. In Sec. IV we present the results of our electrodynamic simulation of the absorption spectrum, taking account of all essential features of the actual composite structure studied in Ref. 1. Conclusions are presented in Sec. V, along with a description of problems that still need to be resolved.

## II. SIMPLE MODEL OF A RESONANT SURFACE LAYER

To examine the essential physics of energy transformation in the system we employ the simplest phenomenological model of a resonant surface layer here in Sec. II. Since the vertical dimensions and the period of the laterally periodic FET structure under consideration (Fig. 1) are much smaller than THz radiation wavelength, we can treat the whole structure as a single plane with a surface admittance of the form

$$Y_{\text{eff}}(\omega) = \sum_{n=0}^{\infty} Y_n(\omega) = -i\bar{\sigma}_0 \sum_{n=0}^{\infty} \frac{2\beta_n^2 \omega \gamma_e}{\omega^2 - \omega_{pn}^2 - 2i\gamma_e \omega}, \quad (1)$$

where  $\bar{\sigma}_0$  is the surface dc conductivity averaged over the period of the structure,  $\omega_{pn}$  is the frequency of the  $n$ th plasma resonance,  $\gamma_e = 1/2\tau$  is the broadening of the resonance caused by electron scattering in the QWs with a phenomenological relaxation time  $\tau$ , and  $\beta_n^2$  is the strength of coupling between the incident THz electromagnetic wave of frequency  $\omega$  and the  $n$ th plasmon mode. A similar approach was used in Refs. 10 and 11 that describes plasmon response in a single 2DEG layer with a metal grating coupler. Assuming  $\omega_0 = 0$  and  $\beta_0^2 = 1$  we have the zeroth term in series equation (1) as the Drude background admittance,

$$Y_0(\omega) = -i\bar{\sigma}_0 \frac{2\gamma_e}{\omega - 2i\gamma_e}.$$

Conventional Fresnel formulas immediately yield the reflectivity and transmittivity of the system as

$$T = \frac{4\sqrt{\varepsilon_1 \varepsilon_2}}{(Z_0 Y_{\text{eff}} + \sqrt{\varepsilon_1} + \sqrt{\varepsilon_2})(Z_0 Y_{\text{eff}}^* + \sqrt{\varepsilon_1} + \sqrt{\varepsilon_2})},$$

$$R = \frac{[(\sqrt{\varepsilon_2} + Z_0 Y_{\text{eff}})^2 - \varepsilon_1][(\sqrt{\varepsilon_2} + Z_0 Y_{\text{eff}}^*)^2 - \varepsilon_1]}{(Z_0 Y_{\text{eff}} + \sqrt{\varepsilon_1} + \sqrt{\varepsilon_2})(Z_0 Y_{\text{eff}}^* + \sqrt{\varepsilon_1} + \sqrt{\varepsilon_2})^2}, \quad (2)$$

where  $\varepsilon_1$  and  $\varepsilon_2$  are the dielectric constants of the adjoining media above and below the resonant surface layer (medium 1 and medium 2, respectively), and  $Z_0$  is the free space impedance. In the vicinity of the  $n$ th plasma resonance,  $\omega \approx \omega_{pn}$ , the  $n$ th term dominates in series (1) and we have

$$Y_{\text{eff}}(\omega) \approx Y_n(\omega) \approx -i\bar{\sigma}_0 \frac{\beta_n^2 \gamma_e}{\omega - \omega_{pn} - i\gamma_e}. \quad (3)$$

Substitution of Eq. (3) for  $Y_{\text{eff}}(\omega)$  into Eqs. (2) yields the transmittivity  $T_n(\omega)$  and reflectivity  $R_n(\omega)$  in the neighborhood of the  $n$ th plasma resonance as

$$T_n(\omega) \approx T_0 \frac{(\omega - \omega_{pn})^2 + \gamma_e^2}{(\omega - \omega_{pn})^2 + (\gamma_e + \gamma_{rn})^2},$$

$$R_n(\omega) \approx R_0 \frac{(\omega - \omega_{pn})^2 + (\gamma_e + \gamma_{rn}/\sqrt{R_0})^2}{(\omega - \omega_{pn})^2 + (\gamma_e + \gamma_{rn})^2},$$

where

$$T_0 = \frac{4\sqrt{\varepsilon_1 \varepsilon_2}}{(\sqrt{\varepsilon_1} + \sqrt{\varepsilon_2})^2}$$

and

$$R_0 = \frac{(\sqrt{\varepsilon_2} - \sqrt{\varepsilon_1})^2}{(\sqrt{\varepsilon_1} + \sqrt{\varepsilon_2})^2}$$

are the transmittivity and reflectivity in the case where there is no resonant surface layer ( $Y_{\text{eff}} = 0$ ) at the interface between medium 1 and 2, and

$$\gamma_{rn} = \bar{\sigma}_0 \gamma_e \frac{Z_0 \beta_n^2}{\sqrt{\varepsilon_1} + \sqrt{\varepsilon_2}}.$$

If we ignore electron scattering in QWs ( $\gamma_e = 0$ ), then the full linewidth of the  $n$ th transmittivity and/or reflectivity resonance would be given by the value of  $\gamma_{rn}$ ; correspondingly,  $\gamma_{rn}$  describes the radiative broadening of the plasma resonance. Since the product  $\bar{\sigma}_0 \gamma_e$  does not depend on electron scattering, one may think of the radiative broadening of the plasma resonance as the parameter that describes coupling between the incident THz wave and the  $n$ th plasmon mode.

The absorbance,  $A_n = 1 - R_n - T_n$ , is given by the above equations having a Lorentzian line shape of

$$A_n(\omega) = \frac{2\gamma_e \gamma_{rn} (1 - \sqrt{R_0})}{(\omega - \omega_{pn})^2 + (\gamma_e + \gamma_{rn})^2},$$

with the total broadening  $\gamma_e + \gamma_{rn}$ . At resonance,  $\omega = \omega_{pn}$ , it is given by

$$A_{\text{res}} = \frac{2\gamma_e \gamma_{rn}}{(\gamma_e + \gamma_{rn})^2} (1 - \sqrt{R_0}).$$

It is readily seen that  $A_{\text{res}} \leq 0.5$  for any values of  $\gamma_e$ ,  $\gamma_{rn}$ , and  $R_0$ . The maximum value,  $A_{\text{res}}^{\text{max}} = 0.5(1 - \sqrt{R_0})$ , occurs when

$\gamma_e = \gamma_{rn}$ . Furthermore, we can consider two limiting cases:  $A_{\text{res}} \approx 2(1 - \sqrt{R_0})\gamma_{rn}/\gamma_e$  when  $\gamma_e \gg \gamma_{rn}$  and  $A_{\text{res}} \approx 2(1 - \sqrt{R_0})\gamma_e/\gamma_{rn}$  when  $\gamma_e \ll \gamma_{rn}$ . It should be noted that there are inverted dependencies of  $A_{\text{res}}$  on the ratio  $\gamma_e/\gamma_{rn}$  in these two limiting cases.

Within the framework of this simple model of a surface resonant layer, the plasmon frequencies,  $\omega_{pn}$ , and radiative broadening,  $\gamma_{rn}$ , are phenomenological parameters to be fitted to their experimental values or to be calculated from a first principles electromagnetic approach.

### III. SINGLE DENSITY-MODULATED 2DEG LAYER

The metal grating gate used in the experiments in Ref. 1 produces electron density modulation in both QWs of the double-quantum-well structure. In addition, the metal grating having period  $L$  couples THz radiation to plasmon modes with in-plane wave vectors  $2\pi n/L$ , with  $n$  an integer.<sup>10–12</sup> In fact, all these wave vectors correspond to zero wave vector in the reduced zone scheme of the periodic structure. The frequencies of these plasmon modes with zero reduced wave vector increase with an increase of  $n$ .<sup>12</sup>

Once induced, the electron density modulation itself can couple THz radiation to plasmon modes even without considering the coupling role of the metal grating. Such “self-coupling” may be more important than metal grating coupling since the metal grating is located a large distance from the 2DEGs in the DQW. To distinguish the effects of self-coupling from those of metal grating coupling, we consider here in Sec. III the absorption of THz radiation power in a density modulated DQW structure without the metal grating.

The separation between the centers of the two QWs in the DQW structure studied in Ref. 1 (27 nm) is two orders of magnitude less than the period of the structure and the wavelength of plasmons excited by the incident THz radiation. Accordingly, we examine a model of the DQW as a *single* 2DEG layer having the combined electron density of the two wells in Ref. 1, located at the interface between the two adjoining dielectric media with dielectric constants  $\epsilon_1$  and  $\epsilon_2$ . In the context of this model, we ignore the bilayer acoustic plasmon modes<sup>13,14</sup> of the system.

We assume a rectangular profile for the surface electron density distribution in the  $x$  direction of the single 2DEG layer under consideration, given by

$$N_s(x) = \begin{cases} N_A & \text{for } 0 < x < w, \\ N_B & \text{for } w < x < L, \end{cases}$$

where  $L$  is the period of the structure. To analyze this system we employ a first principles electromagnetics approach elaborated upon in Ref. 15. In this approach, the integral equation for the surface electron current density in the plane of the 2DEG is developed and studied in terms of a set of orthogonal basis functions, yielding an infinite system of linear algebraic equations which is truncated and solved numerically within a desired level of convergence. The response of the 2DEG is described by a local surface conductivity in Drude form,

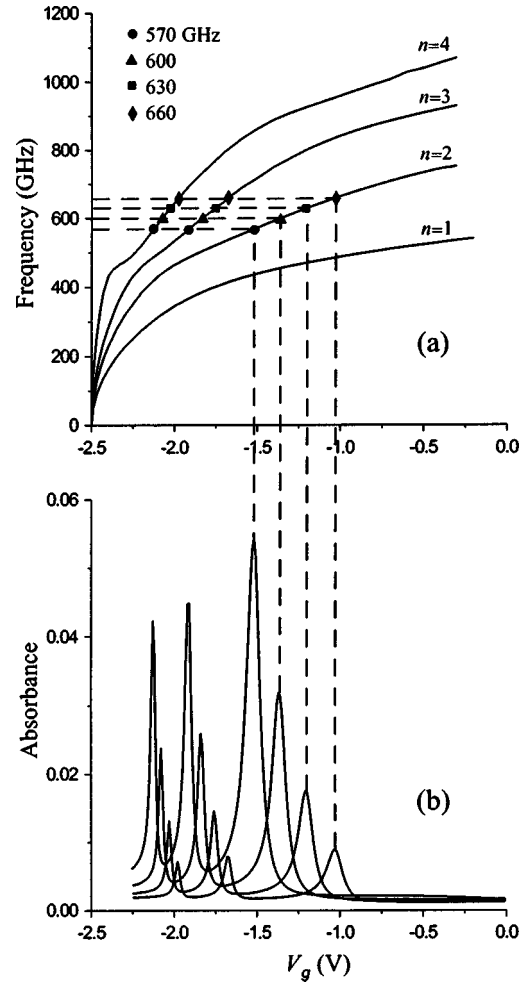


FIG. 2. (a) Frequencies of the lower order plasmon modes and (b) the associated absorption resonances as functions of the gate voltage. Sets of resonances for the second, third, and fourth plasmon modes are shown.  $V_{\text{th}} = -2.5$  V,  $L = 4$   $\mu\text{m}$ ,  $w = 2$   $\mu\text{m}$ .

$$\sigma_{A(B)} = \frac{e^2 N_{A(B)}}{m^*} \frac{\tau}{1 - i\omega\tau},$$

where  $e$  and  $m^*$  are the electron charge and effective mass, respectively, and  $\tau$  is a phenomenological electron relaxation time.

Following the results of Ref. 16, as the modulation factor,  $\Delta n_s = |N_A - N_B|/(N_A + N_B)$ , approaches unity, the spectrum of plasmons at spatial harmonics of the periodically modulated electron gas moves towards lower frequency, but with oscillator strengths that grow for the higher spatial harmonics. Correspondingly, higher plasmon modes,  $n > 1$ , become sequentially more optically active with an increase of  $\Delta n_s$ .

In Fig. 2(a) we exhibit the frequencies of four ( $n = 1, 2, 3, 4$ ) plasmon modes as functions of the modulation factor for characteristic parameters of the actual GaAs/AlGaAs DQW FET structure studied in Ref. 1:  $\epsilon_1 = \epsilon_2 = \epsilon = 12.24$ ,  $m^* = 0.069m_e$ , where  $m_e$  is the free electron mass. The electron density,  $N_A = 4.27 \times 10^{11} \text{ cm}^{-2}$ , is kept unchanged while  $N_B$  varies as a function of the gate voltage  $V_g$  ( $N_B$  decreases with an increase of  $|V_g|$ ). The dependence of



$N_B(V_g)$  was obtained from a parallel plate capacitor model with the gate voltage threshold value,  $V_{th}$ , chosen as a fitting parameter to the experimental data of Ref. 1 (and with zero-gate-voltage electron density in a single 2DEG layer given by  $N_B|_{V_g=0}=N_A$ ). This electrostatics problem was solved separately, and the  $N_B$  value obtained was used as an input parameter in our electrodynamic modeling of the structure without a metal grating.

Figure 2(b) shows the resonant absorption of incident THz electromagnetic radiation at several frequencies. In our calculations we used a fitting parameter  $\tau=8.5\times 10^{-12}$  s. This is roughly an order of magnitude less than the value extracted from the dc mobility. Although the measurement temperatures are substantially above that used to measure the dc mobility, it is not likely that the dc mobility has dropped by an order of magnitude. On the other hand, one may consider inhomogeneous broadening of the plasma resonance: the mean free time for a carrier to traverse a half period of the modulation is  $\sim L/v_F$ , where  $v_F$  is the Fermi velocity of electrons in the QWs, yielding  $\sim 10^{-11}$  s for characteristic parameters of the structure under consideration. This value is of the same order of magnitude as the scattering used to fit the data. It is not productive to pursue this issue further here, but it is possible that a nonlocal description of the conductivity may be more appropriate.

This description of the electrodynamic role of plasmon resonances is more physical than the transmission line model used in Ref. 1, and it leads to better agreement with the experimental observations than that obtained from the latter model.

Figure 3 shows the amplitude of charge and current density oscillations in the plane of the 2DEG layer for the second and third plasmon modes at frequency of 570 GHz. A standing plasma wave appears in the 2DEG strip  $w < x < L$  with lower equilibrium electron density,  $N_B < N_A$ , supporting the speculation in Ref. 1. Note that in our electrodynamic approach, the number of electron density oscillations in this interval is not exactly equal to  $n$ , the plasmon mode index; and the current density is not pinned at the edges of the interval, because the edges of the 2DEG strips with different electron densities are not perfect plasma wave reflectors. However, the dipole-like distribution of nonequilibrium charge density in the 2DEG strip of  $0 < x < w$  with higher equilibrium electron density,  $N_A = \text{const}$ , shown in Fig. 3, is more important. The strength of this dipole controls the optical activity of a given plasmon mode. The charge density and, correspondingly, the  $x$  derivative of the current density distribution, diverge at the edges between 2DEG segments having different equilibrium electron densities as a result of the buildup of edge charges.

The radiative broadenings,  $\gamma_{rn}$ , of the resonances shown in Fig. 2(b), which were estimated from the full linewidth of the transmittivity resonances calculated at  $1/\tau=0$ , are about one tenth the fitted value of  $\gamma_e = 1/2\tau$ .

It is readily seen in Fig. 4 that the optical activity of higher plasmon modes does indeed increase when the modulation factor,  $\Delta n_s$ , tends towards unity (i.e.,  $V_g \rightarrow V_{th}$ ). Therefore, the absorption of THz radiation can be substantially enhanced if one excites higher plasmon modes. The

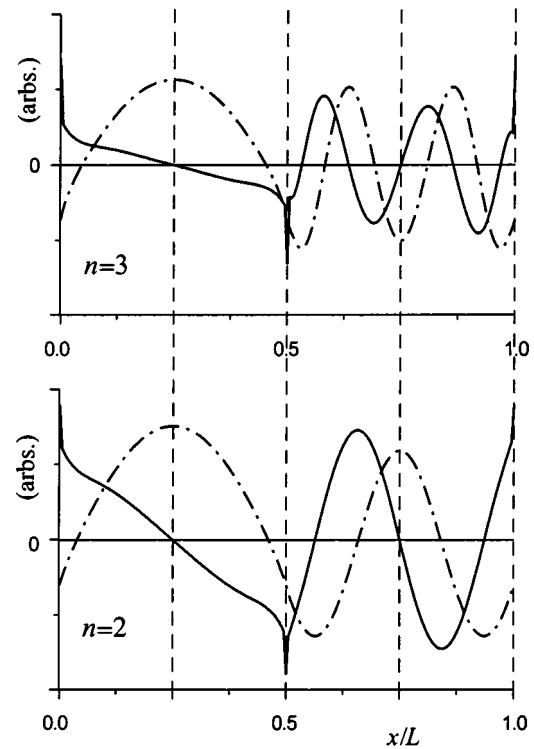


FIG. 3. Amplitude of charge (solid curves) and current (dash-dotted curves) density oscillations over a period of the density-modulated single 2DEG layer for two plasmon modes ( $n=2$  and  $3$ ) at frequency of 570 GHz. The parameters of the structure are the same as those in Fig. 2.

maximum absorbance at resonance for the fourth plasmon mode exceeds 0.3, which is close to the limiting value 0.5 (see Sec. II). Correspondingly, in this case we have  $\gamma_{rn} \approx \gamma_e$ .

In Fig. 4, the plot of absorbance versus gate voltage is used to illustrate the relative absorbance of the  $n=2$  plasmon

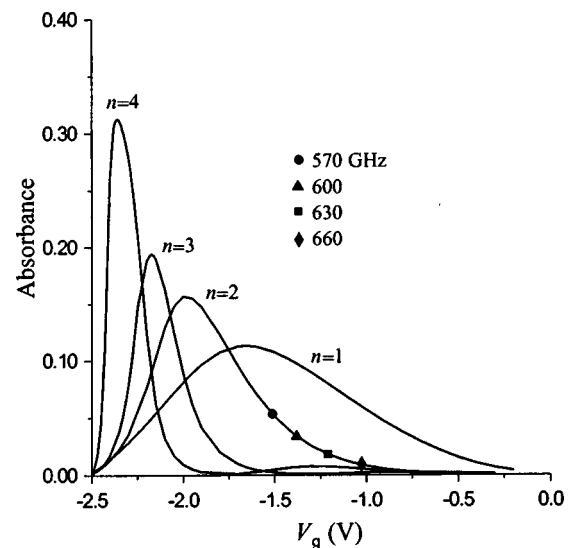


FIG. 4. Absorbance resonances of the first four plasmon modes as functions of the gate voltage. The parameters of the structure are the same as those in Fig. 2. Remarkably, the absorption maxima that occur at different gate voltages for different plasmon modes require nearly the same excitation frequency, which is  $\approx 450$  GHz for parameters relevant to the actual DQW FET structure in Ref. 1.

mode for the four different frequencies used in Ref. 1. These frequencies are seen to resonate at gate voltage far from the the maximum of the absorbance curve for the second plasmon mode. The absorbance maxima at the resonances of the various plasmon modes occur at frequencies which deviate by less than 5% from that of the fundamental dipole mode in the system of isolated 2DEG strips with electron density  $N_A$ . This further corroborates the crucial role of dipole-like oscillations (in the strips of the 2DEG bilayer with higher electron density) in THz absorption processes. The frequency of this dipole mode,  $\omega_{1D}$ , can be estimated from the formula<sup>16</sup>

$$\omega_{1D} = \sqrt{\frac{N_A e^2}{\epsilon_0 \epsilon m^* w}}, \quad (4)$$

where  $\epsilon_0$  is the dielectric permittivity of free space. For the actual characteristic parameters used in our calculations, we have  $\omega_{1D} \approx 450$  GHz. It follows from Eq. (4) that  $\omega_{1D}$  is controlled by both the electron density  $N_A$  and the width of the strips of 2DEG bilayer under the metal grid-gate openings.

#### IV. COMPOSITE DQW FET STRUCTURE

Finally, we address the actual *double*-quantum-well multilayered laterally periodic structure of Ref. 1 here in Sec. IV using a scattering matrix approach<sup>17–19</sup> to analyze all of its essential electrodynamic features and to determine its plasma resonance absorption spectrum. The scattering matrix approach employed involves the following steps: (i) the Maxwell equations are rewritten in an in-plane momentum representation; (ii) then, the electromagnetic eigenmode problem is solved in each layer to obtain a basis set of plane waves that propagate across the layer; (iii) electromagnetic fields in each layer are represented in terms of forward and backward propagating waves; (iv) the scattering matrix of the whole structure is determined using this plane wave representation; and (v) the scattering matrix is then used to calculate reflectivity, transmittivity, and absorbance.

In carrying out this analysis we assume that the effective thicknesses of the upper and lower QWs in the DQW structure are the same, 10 nm each, and that the separation between the center planes of the QWs is 27 nm. We assume that the upper 2DEG is fully depleted under the metallic portions of the grating gate, and forms an array of disconnected  $2 \mu\text{m}$  strips with electron density of  $N_U = 1.7 \times 10^{11} \text{ cm}^{-2}$ . The lower 2DEG is density modulated with  $N_L = 2.57 \times 10^{11} \text{ cm}^{-2}$  essentially unchanged under the strips of the upper 2DEG (i.e., under the open parts of the grating gate). The electron density of the lower 2DEG under metallic portions of the grating gate was obtained from the parallel plate capacitor model described in Sec. III. The metal grating strips are composed of a 20 nm Ti layer covered by a 50 nm Au layer. We took the bulk conductivities as  $\sigma = 2.3 \times 10^4 \text{ S/cm}$  for Ti and  $\sigma = 4.85 \times 10^5 \text{ S/cm}$  for Au. The period of the grating is  $4 \mu\text{m}$  with half the period being metal.

By comparing Figs. 2(b) and 5(a), one can see that the principal absorption resonances in the structure with a metal grating are much stronger than can be attributed to action of the metal grating as the sole coupler. This supports the sug-

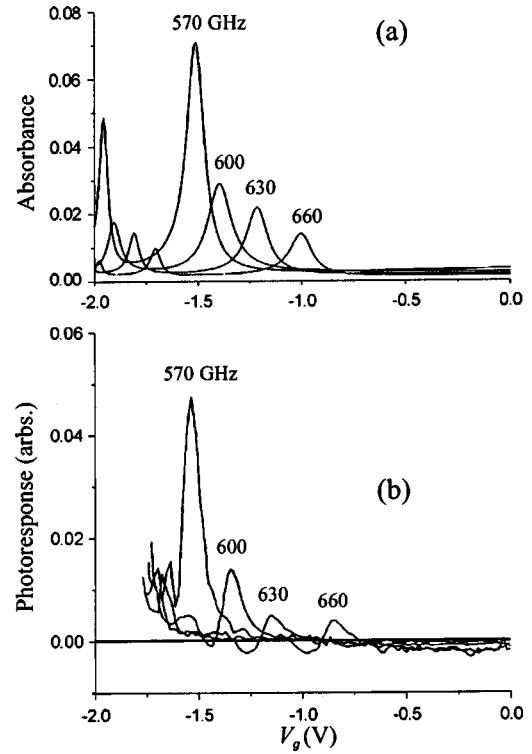


FIG. 5. (a) Calculated absorption spectra of the composite DQW FET structure at several different THz frequencies.  $V_{th} = -2.6$  V is a fitted value. (b) Terahertz photoresponse measured as a function of the gate voltage for four different frequencies at  $T = 25$  K (reported in Ref. 1).

gestion made in Sec. III that the self-coupling effect in a density-modulated 2DEG is more important than metal grating coupling. Moreover, the presence of the metal gate, as well as the finite thickness of the QWs and the QWs separation, leads to relative suppression of the higher frequency absorption resonances. In considering all these issues, it is clear that the variation of line shape with frequency is very close to that observed.

It is worth noting that acoustic plasmon resonances are not manifested in Fig 5(a). This supports our use of the single 2DEG model in Sec. III.

The calculated THz absorption spectra and measured THz photoresponse of two different periods of the DQW FET structure with  $w = L/2$  are shown in Fig. 6. It is evident, for both periods, that the positions of the resonances in photoresponse are related to those of corresponding plasma resonances, although the signs of the photoresponse measurements are opposite for the different periods involved.

It can be seen in Figs. 5 and 6 that the separation between the resonances of THz photoresponse exceeds the calculated separation by about 15%. This difference may be due to the fact that the parallel plate capacitor model we used to calculate the equilibrium electron density in the lower QW suffers by not considering the fringing field effects.

While the resonant positions and strengths are reproduced well by our electrodynamic model, the model has not dealt with the physical mechanism whereby excitation of the plasmon resonances induces changes in the dc transport. The change of sign shown in Fig. 6(b) underscores the fact that this mechanism is not at all understood.

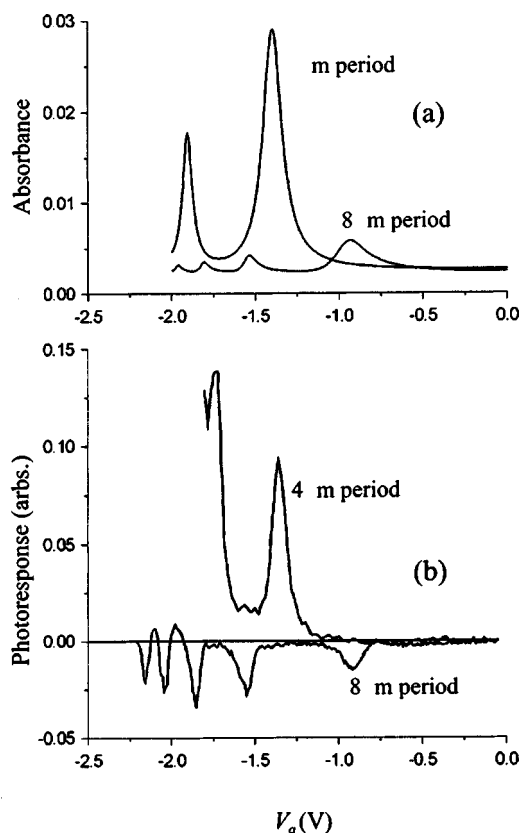


FIG. 6. (a) Calculated absorption spectra of the composite DQW FET structure at frequency of 600 GHz for different periods of the structure. The parameters of the structure are the same as those in Fig. 5. (b) Terahertz photoresponse measured as a function of the gate voltage at frequency of 600 GHz for different periods of the metal gate at  $T = 25$  K.

## V. CONCLUDING REMARKS

We have modeled the absorption spectrum of THz radiation in terms of plasmon modes in a grid-gated DQW FET structure. The simplest model of a surface layer having resonant admittance provided insight into the essential physics of the electromagnetic energy transformation within the system and it showed that the greatest possible absorbance at plasma resonance (which is limited by 0.5) takes place when dissipative broadening of the resonance is equal to its radiative broadening.

Using a numerical simulation of THz absorption in a first principles electromagnetic approach, we have obtained a series of plasma resonances which agree very well with the observed photoresponse resonances in a DQW FET reported recently in Ref. 1. A comparison of the separation between plasma resonances at different THz frequencies obtained from theory with those observed experimentally shows a difference of less than 15%. The model developed here provides firm physics-based theoretical support for the notion that the resonances are related to standing plasmons under the metallic parts of the grating gate. It also shows that the essential feature involved in the absorption spectrum is the density modulation in the channel.

Acoustic plasmons do not seem to influence THz absorption. Modeling absorption by an effective single 2DEG is appropriate in this respect. However, this does not preclude

the possibility that DQW-tunnel-coupled 2DEGs are important in the mechanism that leads to changes in the dc conductance.

We have also shown that higher order spatial harmonics become more optically active as the depth of the electron density modulation in the DQW tends towards unity. The maximum absorbance at high order plasmon mode resonances can approach the limiting value of 0.5.

The frequency of maximum THz absorption at resonance of each plasmon mode is close to the frequency of the fundamental dipole mode in the isolated strips of 2DEG formed when the DQW under metallic portions of the grid gate is fully depleted. A simple evaluation formula for the latter frequency was presented and it provides a useful “rule of thumb” for estimating a set of parameters that will yield enhanced THz absorption of the composite structure.

This theoretical development of the electrodynamics of plasma oscillations in the DQW FET structure was seen to reproduce the experimental observations quite accurately. With this validation, our theoretical approach can be employed to maximize the coupling of THz radiation to grid-gated double-quantum-well field-effect transistors and optimize their performance as incoherent or coherent detectors.

More sophisticated modeling, which takes into account interwell electron transfer in a grid-gated DQW FET structure, is now in progress. We believe that this continuing analysis will provide an even better correspondence between theoretical predictions and experimental results, as well as advance our understanding of the physical mechanism that gives rise to the change in conductance at resonance.

## ACKNOWLEDGMENTS

This work was supported by the Russian Foundation for Basic Research (Grant No. 03-02-17219). The work of two authors (X.G.P. and S.J.A.) was supported by the ONR MFEL program, the DARPA/ONR THz Technology, Sensing and Satellite Communications Program, the ARO through Science and Technology of Nano/Molecular Electronics: Theory, Simulation, and Experimental Characterization, and the Sandia National Laboratory. Sandia is a multiprogram laboratory operated by the Sandia Corporation, a Lockheed Martin Company, for the United States Department of Energy's National Nuclear Security Administration under Contract No. DE-AC04-94AL85000. One author (N.J.M.H.) acknowledges support from the U.S. Department of Defense, Contract No. DAAD 19-01-1-0592. Another author (T.V.T.) thanks INTAS for support (Grant No. YSF 2002-153).

<sup>1</sup>X. G. Peralta, S. J. Allen, M. C. Wanke, N. E. Harff, J. A. Simmons, M. P. Lilly, J. L. Reno, P. J. Burke, and J. P. Eisenstein, *Appl. Phys. Lett.* **81**, 1627 (2002).

<sup>2</sup>X. G. Peralta, S. J. Allen, M. C. Wanke, J. A. Simmons, M. P. Lilly, J. L. Reno, P. J. Burke, and J. P. Eisenstein, *Proceedings of the 26th International Conference on the Physics of Semiconductors*, Ser. 171 (Institute of Physics, Bristol, 2003), E2.3.

<sup>3</sup>S. Katayama, *J. Phys. Soc. Jpn.* **60**, 1123 (1991).

<sup>4</sup>R. J. Wilkinson et al., *J. Appl. Phys.* **71**, 6049 (1992).

<sup>5</sup>S. Katayama, *Surf. Sci.* **263**, 359 (1992).

<sup>6</sup>W. L. Schaich, P. W. Park, and A. H. MacDonald, *Phys. Rev. B* **46**, 12643 (1992).

<sup>7</sup>C. Steinebach, D. Heitmann, and V. Gudmundsson, *Phys. Rev. B* **56**, 6742 (1997).

- <sup>8</sup>S. A. Mikhailov, Phys. Rev. B **58**, 1517 (1998).
- <sup>9</sup>B. P. van Zyl and E. Zaremba, Phys. Rev. B **59**, 2079 (1999).
- <sup>10</sup>S. J. Allen, Jr., D. S. Tsui, and R. A. Logan, Phys. Rev. Lett. **38**, 980 (1977).
- <sup>11</sup>D. S. Tsui, S. J. Allen, Jr., R. A. Logan, A. Kamgar, and S. N. Copper-smith, Surf. Sci. **73**, 419 (1978).
- <sup>12</sup>O. R. Matov, O. V. Polischuk, and V. V. Popov, Int. J. Infrared Millim. Waves **14**, 1455 (1993).
- <sup>13</sup>S. Das Sarma and A. Madhukar, Phys. Rev. B **23**, 805 (1981).
- <sup>14</sup>G. E. Santoro and G. F. Giuliani, Phys. Rev. B **37**, 937 (1988).
- <sup>15</sup>O. R. Matov, O. F. Meshkov, and V. V. Popov, JETP **86**, 538 (1998).
- <sup>16</sup>O. R. Matov, O. V. Polischuk, and V. V. Popov, JETP **95**, 505 (2002).
- <sup>17</sup>C. D. Ager and H. P. Hughes, Phys. Rev. B **44**, 13452 (1991).
- <sup>18</sup>D. M. Whittaker and I. S. Culshaw, Phys. Rev. B **60**, 2610 (1999).
- <sup>19</sup>S. G. Tikhodeev, A. L. Yablonskii, E. A. Muljarov, N. A. Gippius, and T. Ishihara, Phys. Rev. B **66**, 045102 (2002).